Accepted Manuscript

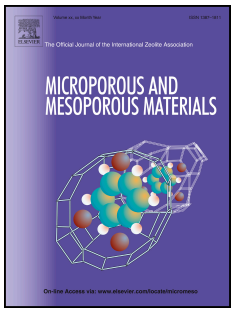

Facile synthesis of Cd-substituted zeolitic-imidazolate framework Cd-ZIF-8 and mixed-metal CdZn-ZIF-8

Jingze Sun, Liya Semenchenko, Woo Taik Lim, Maria Fernanda Ballesteros Rivas, Victor Varela-Guerrero, Hae-Kwon Jeong

PII: S1387-1811(17)30814-4

DOI: 10.1016/j.micromeso.2017.12.032

Reference: MICMAT 8721

To appear in: *Microporous and Mesoporous Materials*

Received Date: 18 October 2017

Revised Date: 27 December 2017

Accepted Date: 28 December 2017

Please cite this article as: J. Sun, L. Semenchenko, W.T. Lim, M.F. Ballesteros Rivas, V. Varela-Guerrero, H.-K. Jeong, Facile synthesis of Cd-substituted zeolitic-imidazolate framework Cd-ZIF-8 and mixed-metal CdZn-ZIF-8, *Microporous and Mesoporous Materials* (2018), doi: 10.1016/j.micromeso.2017.12.032.

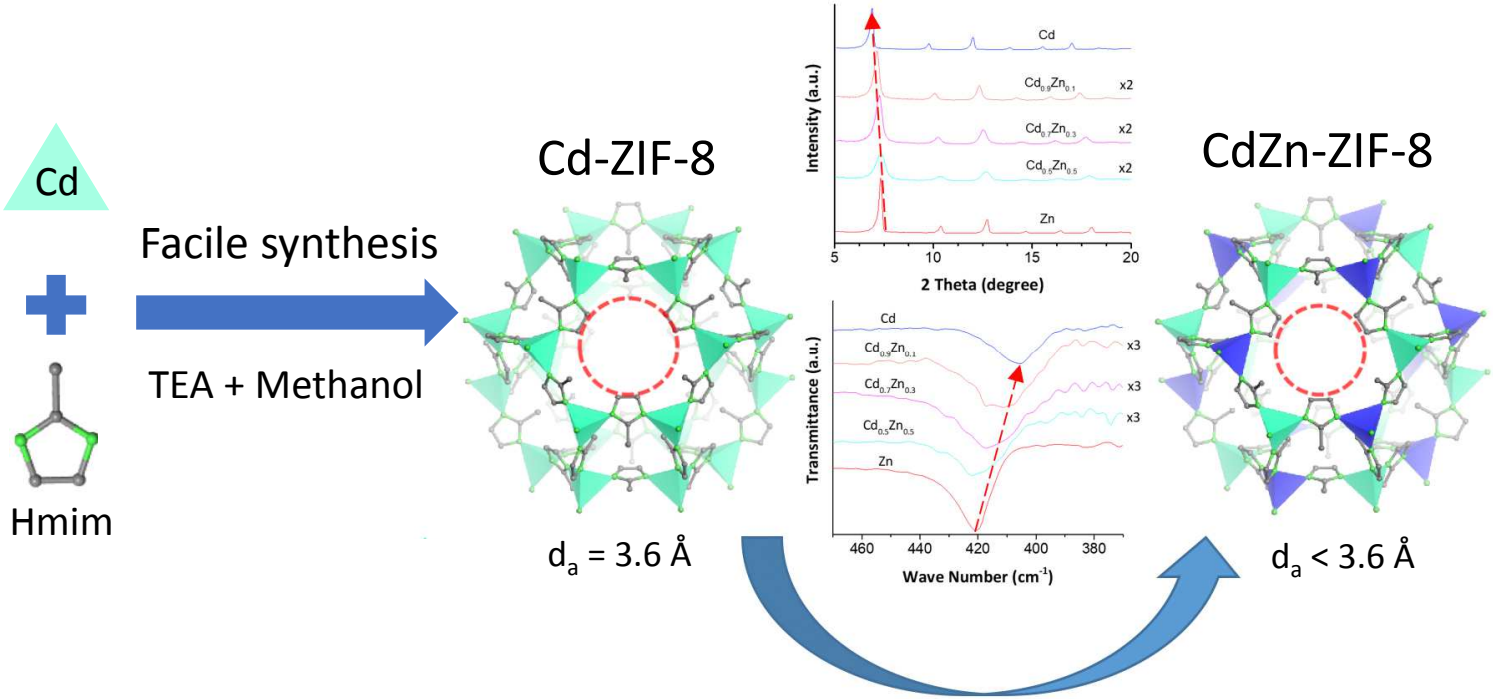
Cd
Hmim
Facile synthesis
TEA + Methanol
Cd-ZIF-8
d_a = 3.6 Å
Intensity (a.u.)
Cd
$Cd_{0.9}Zn_{0.1}$
$Cd_{0.7}Zn_{0.3}$
$Cd_{0.5}Zn_{0.5}$
Zn
x2
5
10
15
20
2 Theta (degree)
Transmittance (a.u.)
x3
460
440
420
400
380
Wave Number (cm^{-1})
CdZn-ZIF-8
d_a < 3.6 Å

Facile Synthesis of Cd-substituted Zeolitic-imidazolate Framework Cd-ZIF-8 and Mixed-metal CdZn-ZIF-8

Jingze Sun,[a] Liya Semenchenko,[b] Woo Taik Lim,[c] Maria Fernanda Ballesteros Rivas,[d] Victor Varela-Guerrero,[d] and Hae-Kwon Jeong†[a, e]

[a]Artie McFerrin Department of Chemical Engineering and [e]Department of Materials Science and Engineering, Texas A&M University, College Station, TX 77843-3122

[b]Department of Chemical Engineering, University of Florida, Gainesville, FL 32611

[c]Department of Applied Chemistry, Andong National University, Andong 36729, Republic of Korea

[d]Centro Conjunto de Investigación en Química Sustentable UAEM-UNAM Universidad Autónoma del Estado de México, Facultad de Química, Paseo Colón S/N, Residencial Colón, 50120 Toluca de Lerdo, México.

†Corresponding author: hjeong7@tamu.edu

ABSTRACT

Zeolitic-imidazole framework ZIF-8 has attracted tremendous interests for the high-resolution kinetic separation of propylene/propane mixture due to its effective aperture size in between the sizes of propylene and propane molecules. It is of great interest to fine-tune the effective aperture size of ZIF-8 either to improve its propylene/propane separation performances or to extend its use to the separation of other gas mixtures. It has been shown that substituting Zn with other metal nodes (e.g. Co) is a potential means to fine-tune the effective aperture size of ZIF-8. Here, we attempt to introduce another metal center, Cd, into ZIF-8 in a facile and scalable manner. Phase-pure Cd-ZIF-8 was successfully synthesized in methanol using a conventional solvothermal method, although it showed a narrow synthesis window. The presence of an organic base (triethylamine, TEA) was found critical not only for the facile synthesis of phase-pure Cd-ZIF-8 but also for the suppression of its phase transformation. A battery of characterizations including single-crystal X-ray structure solutions confirmed that the effective aperture size of Cd-ZIF-8 is the largest among its iso-structures (Zn-ZIF-8 and Co-ZIF-8). Finally, for the first time, mixed-metal CdZn-ZIF-8 crystals with various Cd/Zn ratios were solvothermally synthesized, demonstrating a further opportunity for varying the effective aperture sizes of ZIF-8 and its iso-structures.

Keywords: Zeolitic-imidazolate frameworks, cadmium-imidazolate frameworks, mixed metal MOFs, molecular sieves, gas separation.

1. Introduction

Zeolitic-imidazolate frameworks (ZIFs) [1-10], a subclass of metal-organic frameworks (MOFs), are an emerging class of nanoporous materials comprised of metal nodes and imidazole-derivatives as linkers [1]. Among many ZIFs, ZIF-8 [1], constituted of zinc and 2-methylimidazole (hereafter mIm) forming sodalite (SOD) topology, has been most extensively studied since it possesses robust synthesis protocols, thermal/chemical stability, and well-defined micro-porosity. These unique features of ZIF-8 have greatly facilitated its applications in various fields, including gas separation [11-19], gas storage [20, 21], catalysis [22, 23], and others [24]. Of particular interest is its use in gas separation applications [25, 26]. For example, ZIF-8 has been found extremely effective for the kinetic separation of propylene from propane [13, 27-31].

Substituting zinc nodes in ZIF-8 with other metal nodes (i.e., M-ZIF-8), while keeping the SOD structure, is of great interest not only from a fundamental scientific perspective but also from a practical engineering perspective. For example, partial or complete substitutions of Zn centres in ZIF-8 with catalytically active metals can transform the catalytically inactive ZIF-8 to a catalytically active one [32, 33]. Furthermore, by precisely controlling the metal substitution in ZIF-8, one can potentially fine-tune the effective aperture sizes of ZIF-8 [34], which has significant implications for gas separation applications. ZIF-8 was partially substituted with Cu^{2+} and showed excellent catalytic activity in cyclo-addition reactions, while further doping led to a complete collapse of ZIF-8 structure [32]. ZIF-8 partially doped with Ni^{2+} was synthesized by a mechanochemical method and showed potentials for alcohol sensing and photocatalysis [33]. Kitagawa and his co-workers recently reported both Mg-ZIF-8 [35] and Mn-ZIF-8 [36]. However, the synthesis of both ZIF-8 iso-structures requires delicate conditions (e.g., under Argon) and expensive custom-made reactants ($MgBH_4$ and $MnBH_4$ compounds), attesting to the

challenging nature of metal substitution in ZIF-8. This challenge stems primarily from the fact that ZIF-8 structure requires a nondistorted tetrahedral M-N_4 coordination geometry [36]. More importantly, fully-substituted Mg-ZIF-8 and Mn-ZIF-8 were found not stable in ambient conditions, making them less attractive for practical applications.

On the other hand, fully-substituted Co-ZIF-8 (formerly known as ZIF-67) [1, 7] and Cd-ZIF-8 (formerly known as CdIF-1) [8] are more stable, thereby more interesting from a practical engineering perspective. The synthesis protocol of Co-ZIF-8 is as robust as ZIF-8. Consequently, one can obtain Co-ZIF-8 with various microstructures including particles with their sizes ranging from tens of nanometers to several hundred micrometers as well as supported films, thereby finding its use in various applications including catalysis [37, 38] and gas separations [34, 39]. In contrast, there have been no synthesis protocols reported for the synthesis of Cd-ZIF-8 other than the original single-crystal recipe by Tian et al. [8]. Moreover, the original Cd-ZIF-8 single-crystal synthesis recipe seems not readily applicable for practical applications: large single Cd-ZIF-8 crystals with impurities and the use of n-butanol as solvents. N-butanol is less compatible for the synthesis of mixed-metal ZIF-8 with Cd centres since the synthesis protocols of ZIF-8 and Co-ZIF-8 are mostly based on methanol or water as solvents [40, 41].

Here we report a facile synthesis protocol for phase-pure Cd-ZIF-8 crystals in methanol. Systematic investigations led to synthesis conditions for high-quality Cd-ZIF-8 powder samples. It was revealed that Cd-ZIF-8 has a relative narrow synthesis window and could undergo phase transformations into other phases relatively easily. TEA was found essential not only for the facile synthesis of Cd-ZIF-8 but also for the stabilization of Cd-ZIF-8, preventing phase transformation. With various characterizations, it was found that our Cd-ZIF-8 samples possess thermal stabilities and porosities comparable to its more well-known iso-structures, Zn-ZIF-8

and Co-ZIF-8. Single-crystal structures and FT-IR spectra confirmed that Cd-ZIF-8 possesses larger effective apertures than Zn-ZIF-8. In addition, mixed-metal CdZn-ZIF-8 samples with various Cd/Zn ratios were solvothermally synthesized, showing that Cd substitution can potentially fine-tune the effective aperture size of ZIF-8. It should be noted here that Panda et al. [42] synthesized the first mixed-metal CdZn-ZIF-8 by ball milling but no detailed structural analysis was provided.

2. Experimental

2.1.Chemicals

Cadmium nitrate tetrahydrate (purum p.a., 99+%, Sigma-Aldrich), cadmium acetate dihydrate (purum p.a., 98+%, Sigma-Aldrich), zinc nitrate hexahydrate (98%, Sigma-Aldrich), cobalt nitrate hexahydrate (98%, Sigma-Aldrich), and cobalt chloride (purum p.a. anhydrous, 98+%, Sigma-Aldrich) were used as metal sources. 2-methylimidazole (99%, Sigma-Aldrich) and triethylamine (TEA, 99% reagent grade, Fisher Scientific) were used as an organic ligand and as a deprotonating agent, respectively. Methanol (ACS, absolute, low acetone, 99.8+%, Alfa Aesar) was used for ZIF-8, Co-ZIF-8, and Cd-ZIF-8 powder synthesis. N-butanol (98+%, Fisher Scientific) and dimethylformamide (DMF, 98+%, Fisher Scientific) were used for the synthesis of Cd- and Co-ZIF-8 single crystals, respectively. All these chemicals were used without further purifications.

2.2.Synthesis of Cd-ZIF-8

The molar ratio of Cd:mIm:TEA:methanol in the synthesis precursor solution was 1:x:y:500 where x and y varied from 2 to 8. Reaction times and temperatures were varied from 6 hours to 7

days and from 60 ^{o}C to 110 ^{o}C, respectively. In a typical synthesis, 0.761 g of cadmium nitrate hexahydrate was dissolved in 19.76 g of methanol under stirring to prepare the metal solution. 2 g of TEA and 1.622 g mIm were dissolved into 19.76 g of methanol for the ligand solution. The metal solution was then poured into the ligand solution under stirring and continually stirred for 1 h. The molar ratio of the resulting precursor mixture was Cd:mIm:TEA:methanol = 1:8:8:500. The mixed solution was then transferred into a Teflon-lined autoclave. The autoclave was placed in a convection oven at 60 ^{o}C for 48 h. After the reaction was done, powder was collected, washed with fresh methanol, and dried under vacuum at room temperature.

2.3.Synthesis of Zn-ZIF-8 and Co-ZIF-8

Zn-ZIF-8 powder was synthesized following the recipe reported by Zhang et al.[43] In short, 0.588 g of zinc nitrate hexahydrate was dissolved in 40 ml of methanol. 0.324 g of mIm and 0.538 g of sodium formate were dissolved in 40 ml of methanol. The two solutions were mixed and reacted at 90 ^{o}C for 24 h. The sample was washed twice with fresh methanol and dried in vacuum. Co-ZIF-8 powder was synthesized following a recipe modified from the one by Tang et al.[44] 0.519 g of cobalt chloride was dissolved in 40 ml of methanol while 0.6 g of polyvinylpyrrolidone (PVP) and 2.63 g of mIm were dissolved into another 40 ml of methanol under stirring. These two solutions were mixed and the mixture was then kept at 100 ^{o}C for 12 h. The sample was then washed with fresh methanol twice and dried in vacuum.

2.4.Synthesis of mixed-metal CdZn-ZIF-8

Mixed-metal CdZn-ZIF-8 samples were synthesized based on the Cd-ZIF-8 synthesis protocol described above with slight modifications. The molar ratio of Cd/Zn in the synthesis solution was varied from 9 to 1. After mixing the metal solution containing both zinc salt and

cadmium salt with the ligand solution, the solution was continued stirring for 1 min and then transferred into a Teflon-line autoclave. The reaction was conducted at 60 ^{o}C for 6 h. Gel-like products were collected after centrifuging with 8000 rpm for 20 min, followed by extensive washing in methanol.

2.5.Single crystal synthesis of Zn-ZIF-8, Co-ZIF-8, and Cd-ZIF-8

Zn-ZIF-8 and Co-ZIF-8 single crystals were synthesized according to the recipe reported by Kwon et al.[39] For Zn-ZIF-8 single crystals, 1.764 g of zinc nitrate hexahydrate was dissolved in 20 ml of methanol while 0.973 g of 2-methylimidazole and 0.404 g of sodium formate were dissolved in another 20 ml of methanol. These two solutions were mixed and the resulting mixture was poured into a 45-ml autoclave containing a glass slide and placed in a convection oven at 90 ^{o}C for 6 h. For Co-ZIF-8 single crystals, 1.05 g of cobalt nitrate hexahydrate and 0.27 g of 2-methylimidazole were dissolved in 108 ml of dimethylformamide (DMF) with 6 drops of 1M HNO_3. The two solutions were mixed and the resulting mixture was placed in a convection oven at 130 ^{o}C for 72 h. For Cd-ZIF-8 single crystals, the reported recipe by Tian et al.[8] was slightly modified. 0.267 g of cadmium acetate dihydrate was dissolved in 20 ml of n-butanol and 0.410 g of 2-methylimidazole was dissolved in 15 ml of n-butanol. The latter solution was poured into the former solution. The mixture was put in an autoclave, which was then placed in a convection oven at 120 ^{o}C for 24 h.

2.6.Single-crystal X-ray structures

Diffraction data were collected for these three crystals using synchrotron X-ray. Their temperatures were maintained at 100(1) K by a flow of cold nitrogen gas. Preliminary cell constants and an orientation matrix were determined from 72 sets of frames collected at scan

intervals of 5^o with an exposure time of 1 s per frame. The basic scale file was prepared using the HKL3000 program.[45] The reflections were successfully indexed by the automated indexing routine of the DENZO program [45]. The diffraction data were harvested by collecting 72 sets of frames with 5^o scans with an exposure time of 1 s per frame. These highly redundant data sets were corrected for Lorentz and polarization effects, and a very small correction for crystal decay was applied. The space group $I\bar{4}3m$ was determined by the XPREP program [46]. Full-matrix least-squares refinement (SHELXL2014) [47] was done on F^2 using all data for the three crystals.

2.7.Characterizations

Powder X-ray diffraction (PXRD) patterns were collected from Rigaku Miniflex II powder X-ray diffractometer with Cu-Kα radiation (λ = 1.5406 Å). Field emission scanning electron micrographs were acquired from a JEOL JSM-7500F system operated at an acceleration voltage of 2 keV and a working distance of 15 mm. N_2 adsorption measurements were conducted using a Micrometrics ASAP 2010 system at 77K. FT-IR were collected using a Nicolet 100 FTIR system and potassium bromide was used to form sample mirrors. Thermal gravimetric analysis (TGA) was conducted using a Shimadzu TGA-50 system in the temperate range from room temperature to 600 °C with a ramp rate of 5 °C/min under nitrogen environment. Elemental analysis was performed on an energy dispersive X-ray fluorescence spectrometer (Shimadzu EDX-7000) with a measured range of ^{11}Na to ^{92}U, a 3-mm collimator with a silicon drift detector (SDD). Each sample was analysed under air with the non-destructive quantitative approach. The quantitation method was carried out with an NAVI ® software. The Rh X-ray tube was operated at an excitation voltage and current of 50 kV and 1000 μA, respectively. A spectrum collection time of

1000 s was used per sample. Optical micrographs were taken using an optical microscope (Zeiss Axio Imager A1m).

3. Results and discussion

Fig. 1 shows the PXRD patterns and SEM images of Cd-ZIF-8 crystals with various TEA/Ligand (hereafter, TEA/L) ratios synthesized at 60 ^{o}C for 6 h. The PXRD patterns of Cd-ZIF-8 match well with the simulated one, indicating the powder samples are phase-pure Cd-ZIF-8. The presence of TEA as a deprotonator in the synthesis solution was found essential (unlike Zn-ZIF-8) to synthesize highly crystalline Cd-ZIF-8 powders in methanol (i.e., no precipitates without TEA). It should be mentioned that when water was used as a solvent, only hydroxides of cadmium were formed regardless of the TEA/L ratios, which further illustrates the delicate conditions required for Cd-ZIF-8 synthesis. It is worthy of mentioning here that despite our repeated attempts, it was not possible to synthesize phase-pure Cd-ZIF-8 crystals without any impurities following the recipe by Tian et al. [8] (see Fig. S1).

The use of an organic base to promote the synthesis of MOFs, in particular ZIFs, has been well studied. For example, Gross et al. [40] reported that Zn-ZIF-8 and Co-ZIF-8 crystals could be synthesized even at room temperature in water in the presence of TEA, while Schejn et al. [48, 49] reported the synthesis of ZIF-8 crystals in methanol with TEA. It is noted that even with an excess amount of mIm (mIm to metal molar ratio of as high as 96 in methanol), there were no precipitates formed without TEA. Furthermore, our attempts to use sodium formate (pKa = 7.0 - 8.5), an inorganic deprotonator, failed to produce Cd-ZIF-8 crystals. These observations suggest that TEA plays a key role in the formation of Cd-ZIF-8 crystals.

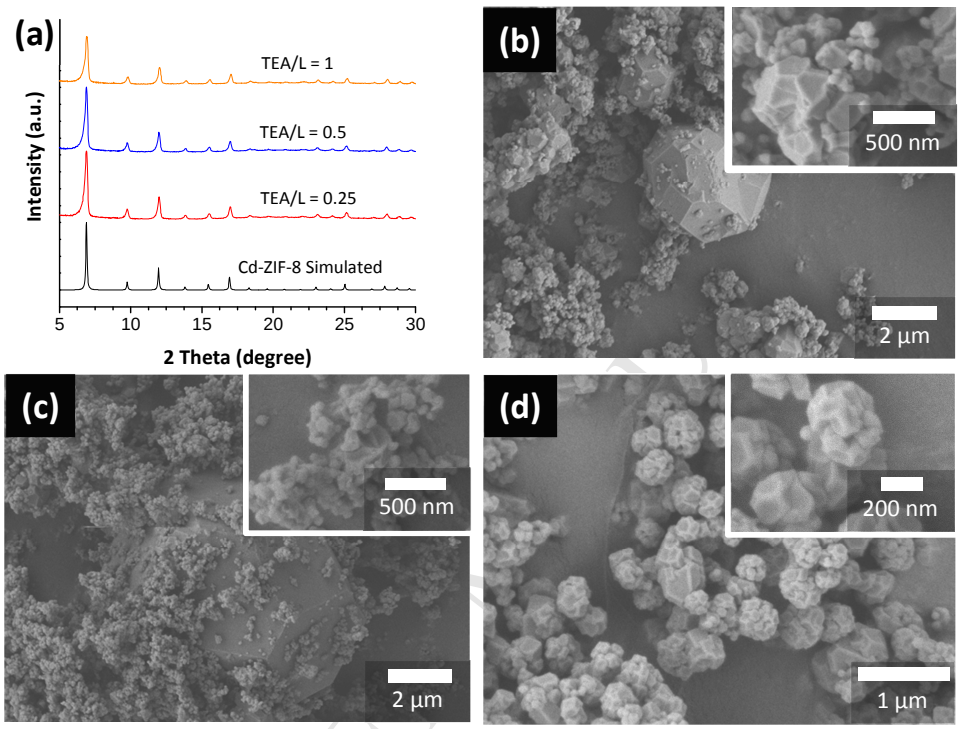

Fig. 1 Cd-ZIF-8 powder samples with different TEA ratios after reactions at 60 ^{o}C for 6 h: (a) PXRD patterns and SEM images of Cd-ZIF-8 samples with the TEA/L of (b) 1, (c) 0.5 and (d) 0.25.

The critical role of TEA likely results from the relatively weak acidity (strong basicity for TEA) of its conjugate acid (pKa = 10.75). Gross et al. [40] showed that the desired values of TEA/L ratios were 1 and 0.5 in water and in methanol, respectively. In our case, no crystal was formed with the TEA/L ratio less than 0.25 in methanol. Unlike Zn^{2+} ions almost always forming tetrahedral coordination, Cd^{2+} ions can form octahedral coordination as well in the presence of

water [50]. Cd^{2+} ions, however, need to be tetrahedrally coordinated (desirably undistorted) to form Cd-ZIF-8 structure. To reduce the coordination number of Cd^{2+} ions to form Cd-ZIF-8 structure, a reconfiguration of the surrounding solvent molecules is required, resulting in an energy barrier [51]. This possibly explains why the synthesis window for Cd-ZIF-8 is much narrower than those for Zn- and Co-ZIF-8, requiring a stronger base to promote the deprotonation of ligands.

Figs. 1b-d show the morphologies of Cd-ZIF-8 crystals prepared with various TEA/L ratios. As can be seen in the SEM images, high TEA/L ratios (> 0.5) appear to promote the formation of crystals with a relatively wider size distribution including micron-sized Cd-ZIF-8 crystals. On the contrary, with the TEA/L of 0.25, crystals are relatively uniform in size of less than 500 nm and no micron-sized crystals can be detected. The majority of the individual Cd-ZIF-8 crystals are nano-sized, looking somewhat different from typical ZIF-8 crystals of similar size. As can be seen in the inset of Fig. 1d, individual crystals seem to be inter-grown to each other, forming agglomerates of similar size. Li et al. [52] observed that many of nano-sized Zn-ZIF-8 and Co-ZIF-8 formed agglomerates when synthesized in the presence of TEA. They attributed this to the high nucleation rates resulting from the presence of TEA, thereby leading to the formation of small crystals.

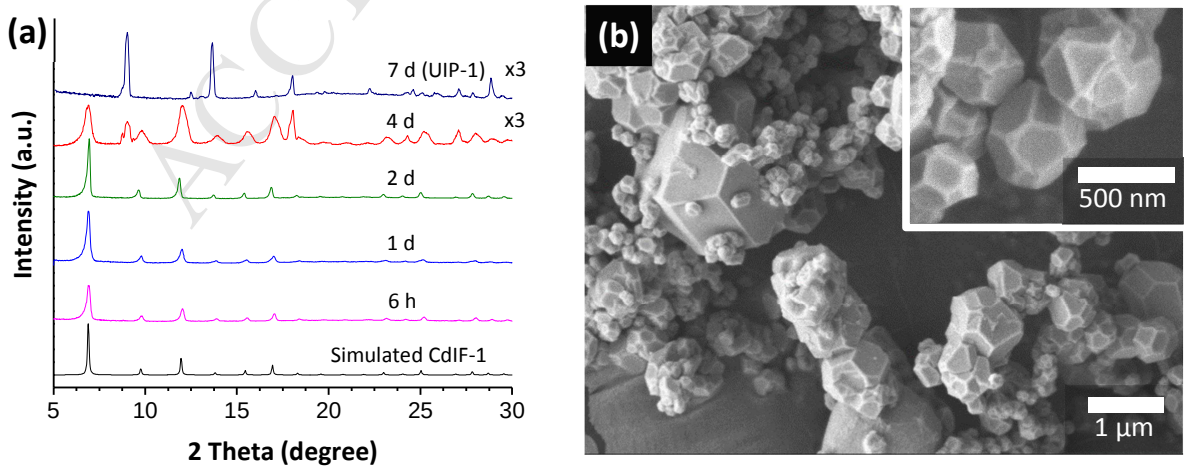

Fig. 2 (a) PXRD patterns for Cd-ZIF-8 with different reaction times and (b) SEM image of powder sample with a reaction time of 2 days. The samples prepared with the molar ratio of Cd:mIm:TEA:MeOH = 1:8:8:500 at 60 ^{o}C

Encouraged by the successful synthesis of phase-pure Cd-ZIF-8 within its narrow synthesis window, the time-dependent formation of Cd-ZIF-8 was studied by varying the synthesis time from 6 h to 7 days. Fig. 2a shows the PXRD patterns of the resulting samples. Cd-ZIF-8 was found undergoing phase changes, which has not been observed in Zn- and Co-ZIF-8 synthesis. As presented in Figs. 2a and S2, the increase in the reaction time led to the improvement in the crystallinity of Cd-ZIF-8 crystals until 2 days. Fig. 2b shows the SEM image of Cd-ZIF-8 crystals synthesized for 2 days, exhibiting much improved morphology as compared to those for 6 h. Further characterizations were carried out with Cd-ZIF-8 crystals synthesized for 2 days. When the reaction time was extended to 4 days, however, there was an unknown phase formed along with Cd-ZIF-8. Furthermore, the crystallinity and morphology of the Cd-ZIF-8 phase synthesized for 4 days were found greatly compromised as shown in Figs. 2a and S2b. Upon 7 days of reaction, an unidentified crystalline impurity phase (hereafter, UIP-1) was observed. This phase change upon elongated reaction time strongly suggests that Cd-ZIF-8 is not as stable as Zn-ZIF-8 and Co-ZIF-8.

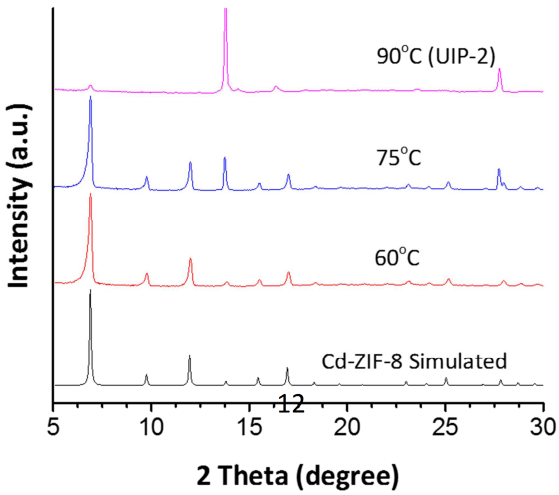

Fig. 3 PXRD patterns of Cd-ZIF powder samples synthesized at different reaction temperatures.

To further explore in the synthesis window, the reaction was conducted from 60 ^{o}C to 130 ^{o}C for 2 days with the Cd:mIm:TEA:MeOH of 1:8:8:500. When the reaction temperature was increased to 75 ^{o}C, an unidentified crystalline impurity phase different from UIP-1 (hereafter, UIP-2) was formed as shown in Figs. 3 and 5b. At 90 ^{o}C, only pure UIP-2 was formed with Cd-ZIF-8 phase. Phase changes upon elevated reaction temperature as well as upon elongated reaction time strongly indicate that Cd-ZIF-8 is not the most thermodynamically stable phase under the current investigated reaction environments, thereby relatively easily transforming to two unknown phases (UIP-1 and UIP-2).

The effect of TEA on the stabilization of Cd-ZIF-8 (i.e., resistance to the phase transformation) was determined by extending the synthesis time (i.e., 2 days) with various TEA/L ratios. As shown in Fig. 4a, with the TEA/L ratio of 0.25, CdIF-3 phase [8] was formed, while with the TEA/L ratio of 0.5, Cd-ZIF-8 formed along with CdIF-3 (see Fig. 4b). When the amount of TEA was further increased (TEA/L = 1), however, phase-pure Cd-ZIF-8 crystals were obtained. This strongly suggests that TEA not only promotes the formation of Cd-ZIF-8 but also stabilizes Cd-ZIF-8 (i.e., prohibiting Cd-ZIF-8 from transforming into CdIF-3).

As described above, Cd-ZIF-8 appears to readily undergo phase transformations into three different phases depending on conditions as summarized in Fig. 5. Careful control over reaction conditions is required to obtain phase-pure Cd-ZIF-8 crystals even in the presence of TEA.

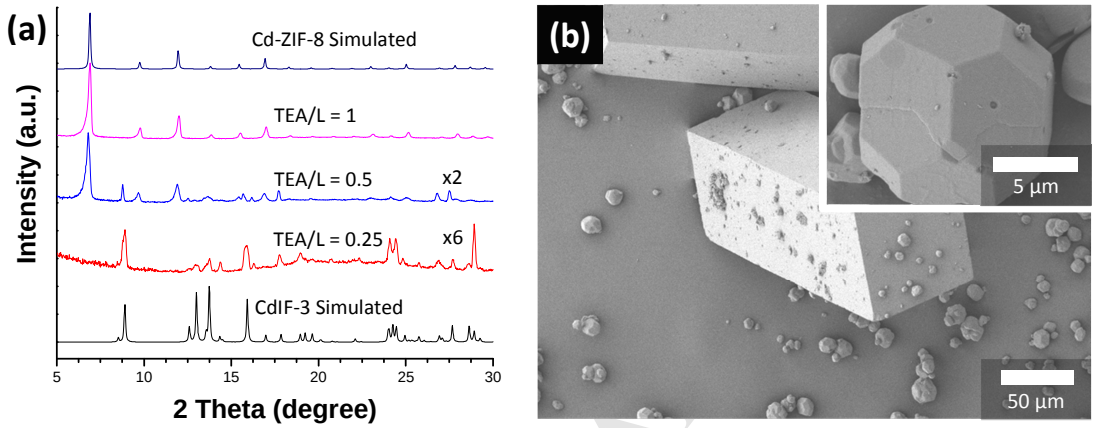

Fig. 4 Cd-ZIF-8 powder samples synthesized with various TEA/L ratios at 60 ^{o}C for 2 days: (a) PXRD patterns and (b) SEM image of the sample with TEA/L = 0.5. Large crystals in rhombic prism shapes are CdIF-3. Inset image shows Cd-ZIF-8 crystals

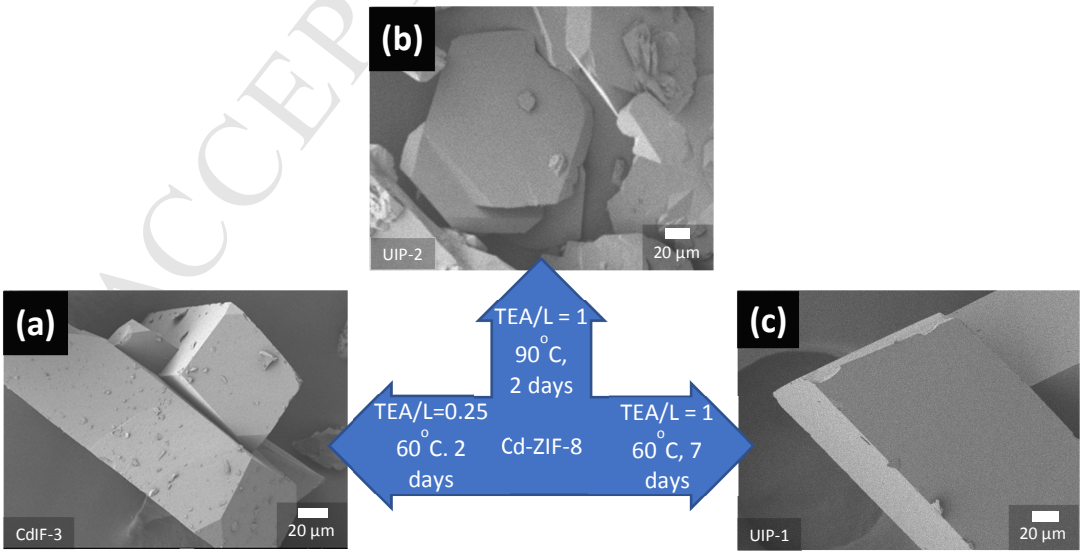

Fig. 5 SEM images of (a) CdIF-3, (b) UIP-2, and (c) UIP-1 and the phase transformation conditions of Cd-ZIF-8 into these three different phases.

Figs. 6 and S3 present the N_2 isotherms of Cd-ZIF-8 in comparison with those of Zn-ZIF-8 and Co-ZIF-8 in semi-log and linear scales, respectively. The isotherms of Zn-ZIF-8 and Co-ZIF-8 exhibit a typical two-step adsorption resulting from the flexibility of the ligands [43, 53]. On the contrary, the isotherm of Cd-ZIF-8 is distinctively different in two ways: 1) only single sharp step around P/P_o ~ 0.00001 and 2) subsequent gradual increase of adsorption without no obvious plateau (i.e., no saturation). This indicates that the flexibility of linkers in Cd-ZIF-8 has less effect on the N_2 adsorption as compared to its iso-structures and a relatively large external surface for Cd-ZIF-8 is present possibly due to the unique morphology of Cd-ZIF-8. As shown in Table 1, Cd-ZIF-8 has much larger external surface area as compared to Zn-ZIF-8 and Co-ZIF-8. It is noted that the Langmuir surface area of Cd-ZIF-8 is slightly lower than that reported by Tian et al. [8] (1985 m²/g vs. 2400 m²/g). The use of TEA in aqueous synthesis often leads to ZIF-8 powders with the BET surface area of ~ 1,000 m^2/g, [40, 49] significantly less than that of ZIF-8 (~ 1,500 m^2/g) [1] prepared in the absence of TEA. This slight decrease in the surface area might be attributed to defects resulting from TEA.

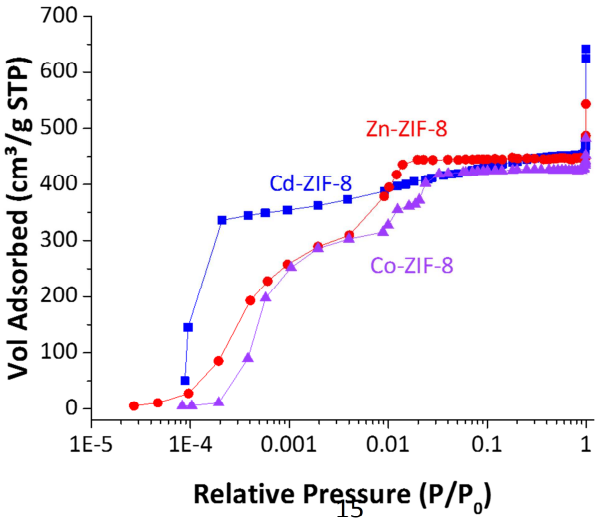

Fig. 6 Nitrogen isotherms (adsorption branches) of Zn-ZIF-8, Co-ZIF-8 and Cd-ZIF-8 at 77 K. Note that the isotherms are presented in a semi-log scale.

The gas diffusion properties of isostructural ZIF-8 structures with different metal centers (i.e., ZIF-8, Co-ZIF-8, and CoZn-ZIF-8) were found dependent on both their crystallographically-defined aperture sizes and the stiffness of the corresponding metal-nitrogen (hereafter, M-N) bonds [34, 39]. M-N distances and metal-mIm-metal (hereafter, M-mIm-M) bond angles are important factors for determining crystallographically-defined aperture sizes. The structure of Cd-ZIF-8 was compared with those of Zn-ZIF-8 and Co-ZIF-8. Since structures solved at different temperatures might lead to differences in bond distances and angles, the single crystal structures of all three ZIF-8 iso-structures were determined under the same conditions at 100 K (see Tables S1-S3 and Fig. S4). Table 2 compared the M-mIm-M bond angles, the M-N bond lengths, and unit cell parameters of three ZIF-8 structures at 100 K (see Fig. S5). While Co-ZIF-8 and Zn-ZIF-8 shares similar bond angles, bond distances, and unit cell parameters, Cd-ZIF-8 shows longer M-N bond length, smaller M-mIm-M angle, and larger cell parameter, thereby exhibiting the largest crystallographically-defined aperture size of ~ 3.6 Å [54].

In addition to the crystallographically-defined aperture size, the effective aperture size is determined by the stiffness of the M-N bonds [14, 55] by affecting the flopping motion of the linkers. For example, if the M-N bonds are more rigid, the flopping motion of the linker is more restricted, thereby resulting in smaller effective aperture. Fig. 7 shows the FT-IR spectra of Zn-ZIF-8, Co-ZIF-8, and Cd-ZIF-8. As compared to the $\nu_{Zn\text{-}N}$, the $\nu_{Co\text{-}N}$ shows a clear blue shift as reported by Kwon et al., [39] while the $\nu_{Cd\text{-}N}$ exhibits a red shift. They attributed the blue shift to the fact that the Co-N bond is mechanically more rigid than the Zn-N bond, leading to the

smaller effective aperture in Co-ZIF-8 [39]. Similarly, the red shift can be caused by the fact that the Cd-N bond is mechanically less rigid than the Zn-N bond in Zn-ZIF-8. In combination with the fact that the crystallographically-defined aperture size of Cd-ZIF-8 is ~ 3.6 Å, the fact that the Cd-N bond is stiffer than the Zn-N and Co-N bonds strongly suggests that its effective aperture is likely much larger than Zn-ZIF-8. It is reasonable to expect Cd-ZIF-8 with its larger effective aperture than ZIF-8 useful for separation of molecules bulkier than propylene and propane.

Table 1 Surface areas and pore volumes of Cd-, Zn- and Co-ZIF-8.

	BET surface area m^2/g	**Langmuir surface area m^2/g**	**Pore volume cm^3/g**	**External surface area m^2/g**
Cd-ZIF-8	1746 ± 11	1985 ± 2	0.5913	218
Zn-ZIF-8	1434 ± 4	1941 ± 4	0.6791	28
Co-ZIF-8	1616 ± 32	1861 ± 2	0.6390	46

Table 2 Topologies, M-N bond distances and unit cell parameters of Cd-, Zn- and Co-ZIF-8, solved from single crystal analysis at 100 K.

	Bond angle M-(mIm)-M /degree	**M-N distance/Å**	**Cell parameter/Å**
Cd-ZIF-8	138.502	2.182(4)	17.902(2)

Zn-ZIF-8	143.714	1.980(2)	16.985(2)
Co-ZIF-8	144.542	1.994(3)	17.003(2)

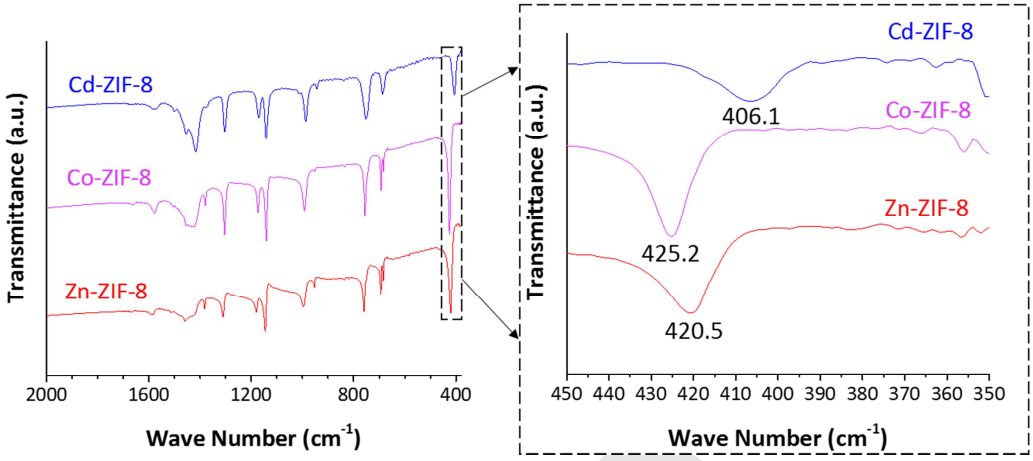

Fig. 7 FT-IR spectra and enlarged spectra (right) of Cd-, Zn- and Co-ZIF-8.

Fig. 8 shows the TGA curves obtained under N_2 for activated Zn-ZIF-8, Co-ZIF-8, and Cd-ZIF-8. It appears that Zn-ZIF-8 and Cd-ZIF-8 are thermally most and least stable, respectively, indicating that the Zn-N and Cd-N bonds are likely to be the strongest and the weakest, respectively.

Finally, ZIF-8 with mixed metal centres (Zn and Cd, hereafter CdZn-ZIF-8) was synthesized to demonstrate the possibility of tuning the effective aperture size of Zn-ZIF-8 by systematically incorporating Cd centers. As the Cd/Zn ratio increases, there were systematic left-shifts in the PXRD peaks (see Fig. 9a) and systematic red-shifts in the M-N stretching bands (see Fig. 9b). Given the fact that the {110} peaks of Cd-ZIF-8 and Zn-ZIF-8 are noticeably separated (by ~ 0.48 degree in 2 theta angles) in combination with the presence of single {110} peaks in CdZn-ZIF-8 samples, it is likely that Cd centres were incorporated into the ZIF-8 frameworks, rather than a simple physical mixture of two structures. When Cd-ZIF-8 and Zn-ZIF-8 were physically

mixed, the mixture exhibited two distinctive {110} peaks (see Fig. S6). Judging from the intensity of the PXRD patterns, our CdZn-ZIF-8 samples are not as crystalline as single-metal ZIF-8. Further synthetic optimization is necessary to improve the crystallinity of CdZn-ZIF-8.

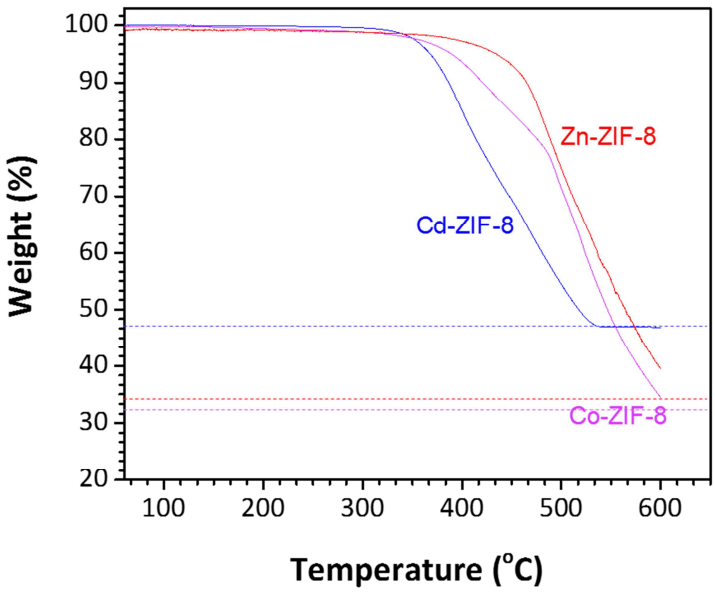

Fig. 8 Thermogravimetric analysis (TGA) curves of Zn-ZIF-8, Co-ZIF-8, and Cd-ZIF-8 performed under N_2. The dotted lines reflected the calculated weight percentage of pyrolyzed metal oxides out of their corresponding ZIFs.

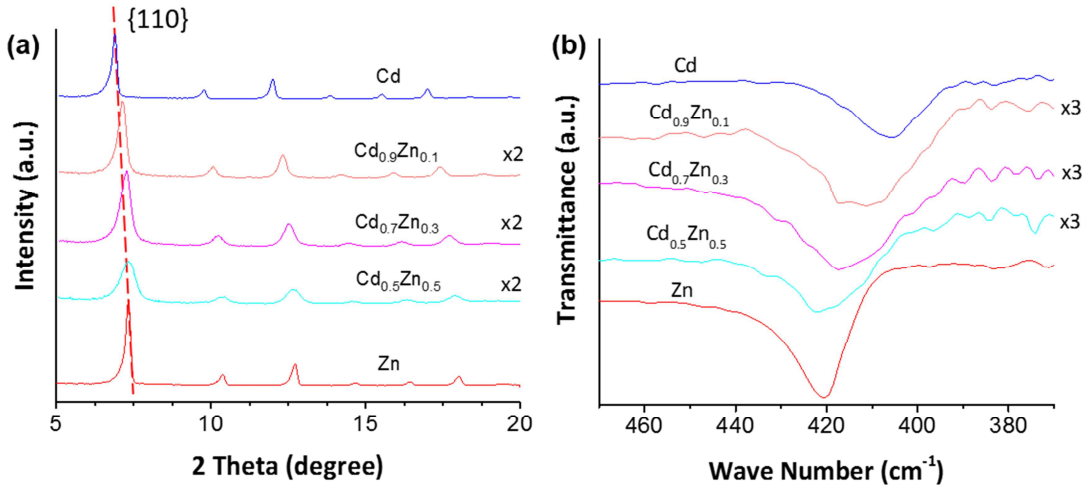

Fig. 9 (a) PXRD patterns and (b) FTIR spectra of CdZn-ZIF-8 with various Cd/Zn ratios in comparison with Cd-ZIF-8 and Zn-ZIF-8. Cd and Zn represents Cd-ZIF-8 and Zn-ZIF-8 while Cd_xZn_{1-x} represents ZIF-8 with x fraction of Cd and (1-x) fraction of Zn in the synthesis solution.

Finally, Table S4 presents the amount of cadmium and zinc metal nodes in CdZn-ZIF-8 determined by elemental analysis. The Zn contents in CdZn-ZIF-8 samples are much higher than those in the synthesis solution. This preferential inclusion of zinc ions is possibly attributed to their smaller size as compared to cadmium ions [50].

3. Conclusion

Phase-pure Cd-ZIF-8 was successfully synthesized using methanol as a solvent. The synthesis window for Cd-ZIF-8 was found much narrower than Zn- and Co-ZIF-8, indicating the meta-stable nature of Cd-ZIF-8 easily undergoing phase transformation into either CdIF-3 or unknown crystalline phases. The presence of TEA was found critical not only for the facile synthesis of phase pure Cd-ZIF-8 but also for the improved resistance of Cd-ZIF-8 to phase transformations. Single crystal structure analysis showed that Cd-ZIF-8 possessed a larger unit cell with the longer M-N bonds compared to both Zn- and Co-ZIF-8, thereby the largest crystallographically-defined aperture (~ 3.6 Å). Furthermore, the Cd-N vibration was red-shifted relative to both Zn-N and Co-N vibrations, suggesting the Cd-N bond is the stiffest. The largest crystallographically-defined aperture in combination of the stiffest Cd-N bond in Cd-ZIF-8 strongly indicate that the effective aperture size of Cd-ZIF-8 is likely to be the largest among three ZIF-8 phases. Finally, the first mixed metal CdZn-ZIF-8 crystals with various Cd/Zn ratios were solvothermally synthesized and shown to exhibit systematic down-shifts in the XRD peaks as well as systematic red-shifts in the M-N vibrations. While the systematic down-shift in the XRD peaks correlate with the systematic increase in the unit cell dimension, the systematic

down-shift in the M-N vibration has to do with the systematic control in the stiffness of the M-N bonds. This ability to systematically control both the unit cell dimension and the M-N bond stiffness by varying the framework Cd/Zn ratio would provide an important means to fine-tune the effective aperture sizes of ZIF-8 iso-structures.

Acknowledgements

H.-K.J. acknowledges the financial support from the National Science Foundation (CMMI-1561897 and CBET-150530) and in part from the Qatar National Research Fund (NPRP 7-042-2-021 and NPRP 8-001-2-001). L.S. appreciates the Undergraduate Summer Research Grant (USRG) from Texas A&M University. The FE-SEM acquisition was supported by the National Science Foundation under Grant DBI-0116835, the VP for Research Office, and the Texas A&M Engineering Experimental Station.

Notes and references

[1] K.S. Park, Z. Ni, A.P. Cote, J.Y. Choi, R.D. Huang, F.J. Uribe-Romo, H.K. Chae, M. O'Keeffe, O.M. Yaghi, Exceptional chemical and thermal stability of zeolitic imidazolate frameworks, PNAS, 103 (2006) 10186-10191.
[2] R. Banerjee, A. Phan, B. Wang, C. Knobler, H. Furukawa, M. O'Keeffe, O.M. Yaghi, High-throughput synthesis of zeolitic imidazolate frameworks and application to CO2 capture, Science, 319 (2008) 939-943.
[3] W. Morris, C.J. Doonan, H. Furukawa, R. Banerjee, O.M. Yaghi, Crystals as molecules: Postsynthesis covalent functionalization of zeolitic imidazolate frameworks, J. Am. Chem. Soc., 130 (2008) 12626-12627.
[4] B. Wang, A.P. Cote, H. Furukawa, M. O'Keeffe, O.M. Yaghi, Colossal cages in zeolitic imidazolate frameworks as selective carbon dioxide reservoirs, Nature, 453 (2008) 207.
[5] D.J. Tranchemontagne, J.R. Hunt, O.M. Yaghi, Room temperature synthesis of metal-organic frameworks: MOF-5, MOF-74, MOF-177, MOF-199, and IRMOF-0, Tetrahedron, 64 (2008) 8553-8557.
[6] H. Hayashi, A.P. Cote, H. Furukawa, M. O'Keeffe, O.M. Yaghi, Zeolite A imidazolate frameworks, Nat. Mater., 6 (2007) 501-506.

[7] Q. Shi, Z. Chen, Z. Song, J. Li, J. Dong, Synthesis of ZIF‐8 and ZIF‐67 by Steam‐Assisted Conversion and an Investigation of Their Tribological Behaviors, Angew. Chem. Int. Ed., 50 (2011) 672-675.
[8] Y.Q. Tian, S.Y. Yao, D. Gu, K.H. Cui, D.W. Guo, G. Zhang, Z.X. Chen, D.Y. Zhao, Cadmium imidazolate frameworks with polymorphism, high thermal stability, and a large surface area, Chemistry, 16 (2010) 1137-1141.
[9] O. Karagiaridi, W. Bury, A.A. Sarjeant, C.L. Stern, O.K. Farha, J.T. Hupp, Synthesis and characterization of isostructural cadmium zeolitic imidazolate frameworks via solvent-assisted linker exchange, Chem. Sci., 3 (2012) 3256-3260.
[10] T.H. Bae, J.S. Lee, W. Qiu, W.J. Koros, C.W. Jones, S. Nair, A High‐Performance Gas‐Separation Membrane Containing Submicrometer‐Sized Metal−Organic Framework Crystals, Angew. Chem. Int. Ed., 49 (2010) 9863-9866.
[11] M. Shah, M.C. McCarthy, S. Sachdeva, A.K. Lee, H.K. Jeong, Current Status of Metal-Organic Framework Membranes for Gas Separations: Promises and Challenges, Ind. Eng. Chem. Res., 51 (2012) 2179-2199.
[12] J.-R. Li, J. Sculley, H.-C. Zhou, Metal–organic frameworks for separations, Chem. Rev., 112 (2011) 869-932.
[13] H.T. Kwon, H.K. Jeong, Highly propylene-selective supported zeolite-imidazolate framework (ZIF-8) membranes synthesized by rapid microwave-assisted seeding and secondary growth, Chem. Commun., 49 (2013) 3854-3856.
[14] C. Zhang, R.P. Lively, K. Zhang, J.R. Johnson, O. Karvan, W.J. Koros, Unexpected Molecular Sieving Properties of Zeolitic Imidazolate Framework-8, J Phys Chem Lett, 3 (2012) 2130-2134.
[15] Y.Y. Liu, G.F. Zeng, Y.C. Pan, Z.P. Lai, Synthesis of highly c-oriented ZIF-69 membranes by secondary growth and their gas permeation properties, J. Membr. Sci., 379 (2011) 46-51.
[16] Y. Pan, Z. Lai, Sharp separation of C2/C3 hydrocarbon mixtures by zeolitic imidazolate framework-8 (ZIF-8) membranes synthesized in aqueous solutions, Chem. Commun., 47 (2011) 10275-10277.
[17] K. Zhang, R.P. Lively, C. Zhang, W.J. Koros, R.R. Chance, Investigating the Intrinsic Ethanol/Water Separation Capability of ZIF-8: An Adsorption and Diffusion Study, J. Phys. Chem. C, 117 (2013) 7214-7225.
[18] H.L. Huang, W.J. Zhang, D.H. Liu, B. Liu, G.J. Chen, C.L. Zhong, Effect of temperature on gas adsorption and separation in ZIF-8: A combined experimental and molecular simulation study, Chem. Eng. Sci., 66 (2011) 6297-6305.
[19] Y.C. Pan, Y.Y. Liu, G.F. Zeng, L. Zhao, Z.P. Lai, Rapid synthesis of zeolitic imidazolate framework-8 (ZIF-8) nanocrystals in an aqueous system, Chem. Commun., 47 (2011) 2071-2073.
[20] L. Mu, B. Liu, H. Liu, Y. Yang, C. Sun, G. Chen, A novel method to improve the gas storage capacity of ZIF-8, J. Mater. Chem., 22 (2012) 12246-12252.
[21] R. Kumar, K. Jayaramulu, T.K. Maji, C. Rao, Hybrid nanocomposites of ZIF-8 with graphene oxide exhibiting tunable morphology, significant CO 2 uptake and other novel properties, Chem. Commun., 49 (2013) 4947-4949.
[22] U.P. Tran, K.K. Le, N.T. Phan, Expanding applications of metal− organic frameworks: zeolite imidazolate framework ZIF-8 as an efficient heterogeneous catalyst for the knoevenagel reaction, ACS Catalysis, 1 (2011) 120-127.

[23] H.-L. Jiang, B. Liu, T. Akita, M. Haruta, H. Sakurai, Q. Xu, Au@ ZIF-8: CO oxidation over gold nanoparticles deposited to metal− organic framework, J. Am. Chem. Soc., 131 (2009) 11302-11303.
[24] G. Lu, J.T. Hupp, Metal− organic frameworks as sensors: a ZIF-8 based Fabry− Pérot device as a selective sensor for chemical vapors and gases, J. Am. Chem. Soc., 132 (2010) 7832-7833.
[25] H. Bux, F. Liang, Y. Li, J. Cravillon, M. Wiebcke, J. Caro, Zeolitic imidazolate framework membrane with molecular sieving properties by microwave-assisted solvothermal synthesis, J. Am. Chem. Soc., 131 (2009) 16000-16001.
[26] M.C. McCarthy, V. Varela-Guerrero, G.V. Barnett, H.K. Jeong, Synthesis of zeolitic imidazolate framework films and membranes with controlled microstructures, Langmuir, 26 (2010) 14636-14641.
[27] Y.C. Pan, T. Li, G. Lestari, Z.P. Lai, Effective separation of propylene/propane binary mixtures by ZIF-8 membranes, J. Membr. Sci., 390 (2012) 93-98.
[28] N. Hara, M. Yoshimune, H. Negishi, K. Haraya, S. Hara, T. Yamaguchi, Diffusive separation of propylene/propane with ZIF-8 membranes, J. Membr. Sci., 450 (2014) 215-223.
[29] C. Zhang, W.J. Koros, Zeolitic imidazolate framework-enabled membranes: challenges and opportunities, J. Phys. Chem. Lett., 6 (2015) 3841-3849.
[30] K. Li, D.H. Olson, J. Seidel, T.J. Emge, H. Gong, H. Zeng, J. Li, Zeolitic imidazolate frameworks for kinetic separation of propane and propene, J. Am. Chem. Soc., 131 (2009) 10368-10369.
[31] D. Liu, X. Ma, H. Xi, Y. Lin, Gas transport properties and propylene/propane separation characteristics of ZIF-8 membranes, J. Membr. Sci., 451 (2014) 85-93.
[32] A. Schejn, A. Aboulaich, L. Balan, V. Falk, J. Lalevée, G. Medjahdi, L. Aranda, K. Mozet, R. Schneider, Cu 2+-doped zeolitic imidazolate frameworks (ZIF-8): efficient and stable catalysts for cycloadditions and condensation reactions, Catal. Sci. Tech., 5 (2015) 1829-1839.
[33] J.-S. Qin, D.-Y. Du, W.-L. Li, J.-P. Zhang, S.-L. Li, Z.-M. Su, X.-L. Wang, Q. Xu, K.-Z. Shao, Y.-Q. Lan, N-rich zeolite-like metal–organic framework with sodalite topology: high CO 2 uptake, selective gas adsorption and efficient drug delivery, Chem. Sci., 3 (2012) 2114-2118.
[34] F. Hillman, J.M. Zimmerman, S.-M. Paek, M.R.A. Hamid, W.T. Lim, H.-K. Jeong, Rapid microwave-assisted synthesis of hybrid zeolitic–imidazolate frameworks with mixed metals and mixed linkers, J. Mater. Chem. A, 5 (2017) 6090-6099.
[35] S. Horike, K. Kadota, T. Itakura, M. Inukai, S. Kitagawa, Synthesis of magnesium ZIF-8 from Mg (BH 4) 2, Dalton Trans., 44 (2015) 15107-15110.
[36] K. Kadota, E. Sivaniah, S. Bureekaew, S. Kitagawa, S. Horike, Synthesis of Manganese ZIF-8 from [Mn (BH4) 2· 3THF]· NaBH4, Inorg. Chem., (2017).
[37] J. Yang, F. Zhang, H. Lu, X. Hong, H. Jiang, Y. Wu, Y. Li, Hollow Zn/Co ZIF Particles Derived from Core‐Shell ZIF‐67@ ZIF‐8 as Selective Catalyst for the Semi‐Hydrogenation of Acetylene, Angew. Chem. Int. Ed., 54 (2015) 10889-10893.
[38] H. Yang, X.-W. He, F. Wang, Y. Kang, J. Zhang, Doping copper into ZIF-67 for enhancing gas uptake capacity and visible-light-driven photocatalytic degradation of organic dye, J. Mater. Chem., 22 (2012) 21849-21851.
[39] H.T. Kwon, H.K. Jeong, A.S. Lee, H.S. An, J.S. Lee, Heteroepitaxially grown zeolitic imidazolate framework membranes with unprecedented propylene/propane separation performances, J. Am. Chem. Soc., 137 (2015) 12304-12311.

[40] A.F. Gross, E. Sherman, J.J. Vajo, Aqueous room temperature synthesis of cobalt and zinc sodalite zeolitic imidizolate frameworks, Dalton Trans., 41 (2012) 5458-5460.
[41] M. He, J.F. Yao, Q. Liu, K. Wang, F.Y. Chen, H.T. Wang, Facile synthesis of zeolitic imidazolate framework-8 from a concentrated aqueous solution, Microporous Mesoporous Mater., 184 (2014) 55-60.
[42] T. Panda, S. Horike, K. Hagi, N. Ogiwara, K. Kadota, T. Itakura, M. Tsujimoto, S. Kitagawa, Mechanical Alloying of Metal–Organic Frameworks, Angew. Chem., 129 (2017) 2453-2457.
[43] C. Zhang, J.A. Gee, D.S. Sholl, R.P. Lively, Crystal-Size-Dependent Structural Transitions in Nanoporous Crystals: Adsorption-Induced Transitions in ZIF-8, J. Phys. Chem. C, 118 (2014) 20727-20733.
[44] J. Tang, R.R. Salunkhe, J. Liu, N.L. Torad, M. Imura, S. Furukawa, Y. Yamauchi, Thermal conversion of core-shell metal-organic frameworks: a new method for selectively functionalized nanoporous hybrid carbon, J. Am. Chem. Soc., 137 (2015) 1572-1580.
[45] W. Minor, M. Cymborowski, Z. Otwinowski, M. Chruszcz, HKL-3000: the integration of data reduction and structure solution--from diffraction images to an initial model in minutes, Acta Crystallogr. Sect. D. Biol. Crystallogr., 62 (2006) 859-866.
[46] Bruker, XPREP Program (ver. 6.12), Bruker AXS Inc., Madison, Wisconsin, USA, 2001.
[47] G.M. Sheldrick, A short history of SHELX, Acta Crystallogr A, 64 (2008) 112-122.
[48] A. Schejn, L. Balan, V. Falk, L. Aranda, G. Medjahdi, R. Schneider, Controlling ZIF-8 nano- and microcrystal formation and reactivity through zinc salt variations, Crystengcomm, 16 (2014) 4493-4500.
[49] N.A.H.M. Nordin, A.F. Ismail, A. Mustafa, R.S. Murali, T. Matsuura, The impact of ZIF-8 particle size and heat treatment on CO2/CH4 separation using asymmetric mixed matrix membrane, RSC Adv., 4 (2014) 52530-52541.
[50] E.C. Constable, Zinc and Cadmium, Coord. Chem. Rev., 58 (1984) 1-51.
[51] J.J. Birger, Cadmium-imidazole complex formation in aqueous solutions, stability constants, changes in standard free energies, enthalpies, entropies, and heat capaciites accompanying the complex formation at 5, 15, 25 and 40 C. , Acta Chem. Scand. A, 29 (1975) 250-254.
[52] Y. Li, K. Zhou, M. He, J.F. Yao, Synthesis of ZIF-8 and ZIF-67 using mixed-base and their dye adsorption, Microporous Mesoporous Mater., 234 (2016) 287-292.
[53] D. Fairen-Jimenez, S.A. Moggach, M.T. Wharmby, P.A. Wright, S. Parsons, T. Duren, Opening the Gate: Framework Flexibility in ZIF-8 Explored by Experiments and Simulations, J. Am. Chem. Soc., 133 (2011) 8900-8902.
[54] P. Krokidas, M. Castier, I.G. Economou, A Computational Study of ZIF-8 and ZIF-67 Performance for Separation of Gas Mixtures, J. Phys. Chem. C, 121 (2017) 17999-18011.
[55] P. Krokidas, M. Castier, S. Moncho, D.N. Sredojevic, E.N. Brothers, H.T. Kwon, H.-K. Jeong, J.S. Lee, I.G. Economou, ZIF-67 Framework: A Promising New Candidate for Propylene/Propane Separation. Experimental Data and Molecular Simulations, J. Phys. Chem. C, 120 (2016) 8116-8124.

Highlights

- A facile synthesis of phase-pure Cd-ZIF-8 is developed
- Cd-ZIF-8 is meta-stable, readily transforming to other phases
- Tetraethylamine is critical for obtaining and stabilizing Cd-ZIF-8
- First mixed-metal CdZn-ZIF-8 is synthesized